Revista Brasileira de Geofísica
RBGf
Brazilian Journal of Geophysics

Revista Brasileira de Geofísica (2013) 31(1): 31-41

ISSN 0102-261X
www.scielo.br/rbg

PLANETARY-SCALE CLIMATIC INDICES AND RELATIONSHIP BETWEEN DECADAL VARIABILITY OF RAINFALL IN NORTHEASTERN AND SOUTHERN BRAZIL

Luciana Figueiredo Prado and Ilana Wainer

ABSTRACT. This work analyzes the relationship between climatic indicies and rainfall in the Northeastern (NE) and Southern (S) Brazil, in decadal timescale. The climatic indicies were obtained from the reanalysis data from NCEP/NCAR (National Centers for Environmental Prediction/National Center for Atmospheric Research) between 1948 and 2008. Subsequently, we calculated the correlation coefficients between the indices and GPCP (Global Precipitation Climatology Project) precipitation anomalies using filtered and non-filtered time series, within the decadal frequency. The results show that El Niño Southern Oscillation (ENSO) is the main phenomenon influencing NE rainfall due to related changes in tropical circulation while the Intertropical Convergence Zone (ITCZ) annual cycle also affects rainfall in the NE to a lesser extent. Meanwhile, in the Southern region, the most important phenomenon is the Southern Annular Mode (SAM) which controls cyclones activity in mid-latitudes. The Tropical Atlantic dipole index (ADI) also influences the rainfall in the Southern, and this might be related to moisture being transported from the ocean to the continent, which is then carried to the South by the Low Level Jet. It is also suggested that the decadal variability of the Tropical Atlantic Ocean and its influence on the precipitation in NE and S regions of Brazil are episodic because no significant correlations were obtained at decadal frequency. Finally, the spectral analysis revealed that the interannual timescale is the main frequency of variability in both studied regions, affecting differently each one of them.

Keywords: rainfall, ENSO, Atlantic, SAM.

RESUMO. Este trabalho analisa as relações entre índices climáticos e a precipitação no Nordeste (NE) e Sul (S) do Brasil, em escala decadal. Os índices climáticos foram obtidos a partir de dados da reanálise do NCEP/NCAR (National Centers for Environmental Prediction/National Center for Atmospheric Research), para o período de 1948 a 2008. Posteriormente, foram obtidos os coeficientes de correlação entre os índices e as anomalias de precipitação advindas do banco de dados do GPCP (Global Precipitation Climatology Project) nestas regiões, utilizando séries não filtradas e séries filtradas na frequência decadal. Os resultados sugerem que o principal fenômeno que modula a precipitação no NE é o El Niño-Oscilação Sul (ENOS), devido às alterações na circulação tropical, e também o ciclo anual da Zona de Convergência Intertropical (ZCIT), que modula a estação chuvosa do NE. Na região S, o fenômeno que mais influencia a precipitação em escala decadal é o Modo Anular Sul (SAM), por modular a atividade ciclogenética em latitudes médias, além do índice do dipolo do Atlântico Tropical (DA), que pode estar ligado ao aporte de umidade oceânica para o continente, e levada ao S pelo jato de baixos níveis. Também se sugere que a variabilidade decadal do Atlântico tropical e sua influência na precipitação no NE sejam episódicas, e não periódica, já que não foram obtidas correlações importantes para este índice, na frequência estudada. Finalmente, a análise espectral revelou que a escala interanual é a principal frequência de variabilidade temporal em ambas as regiões, com efeitos diversos em cada uma delas.

Palavras-chave: precipitação, ENOS, Atlântico, SAM.

Instituto Oceanográfico, Universidade de São Paulo, Praça do Oceanográfico, 191, Cidade Universitária, 05508-120 São Paulo, SP, Brazil. Phone: +55 (11) 3091-6531 – E-mails: luciana.prado@usp.br; wainer@usp.br

INTRODUCTION

General circulation of the global atmosphere physical components varies in different frequencies and interacts on several space and time scales, thus defining the complexity of Earth's climate system. One way to analyze these interactions is by studying teleconnection patterns. Teleconnections (Wallace & Gutzler, 1981) are significant correlations among temporal oscillations of weather patterns occurring far apart on the Earth surface. Typically, such patterns are observed as a stationary wave that are identified with temporal series of climate variables such as temperature and pressure (or a combination of them) for the interest area. These temporal series are correlated, with or without offset, to determine whether there is a signal-response pattern.

One of the first teleconnection pattern observations among the Atlantic Ocean and Europe was made by Van Loon & Rogers (1978), who detected an air mass exchange between the low polar and the high subtropical regions of the North Atlantic. This dipole pressure field at sea level is called the North Atlantic Oscillation (NAO) and is given by the pressure difference between Lisbon, Portugal and Stykkisholmur, Iceland, during boreal winter. The NAO is the leading variability mode in the European winter.

Other teleconnection patterns were identified in several regions around the world. Two main variabilities were identified in the Pacific Ocean. At decadal scale, the deepening of the Aleutian Low in the North Pacific and the consequent warming of the equatorial Pacific define the Pacific Decadal Oscillation (PDO), which affects significantly winter in North America (Mantua et al., 1997). The El Niño-Southern Oscillation (ENSO) consists of interannual variations of Sea Surface Temperature (SST) in the equatorial Pacific, coupled with a seesaw pattern of sea level pressure between Tahiti and Darwin, Australia (Bjerknes, 1966; Trenberth, 1976). This is the main interannual climate variability in South America (Grimm, 2003).

Walker (1928) observed a large-scale alternation pattern of atmospheric mass between middle and high latitudes in the Southern Hemisphere. Such variability is called Antarctic Oscillation or Southern Annular Mode (SAM) and is characterized by the opposite relationship between anomaly signs of sea level pressure centered in Antarctica and in the 40-50°S latitude range (Hall & Visbeck, 2002). In the tropics, studies from the 70's and contemporary (Hastenrath & Heller, 1977; Servain et al., 1999, 2003; Wainer et al., 2003) report a dipole pattern between North (NAT) and South Atlantic Tropical (SAT) SST associated with extreme events in the basin vicinity. Moreover, the equatorial region has an annual cycle in the low pressure region associated with convection called Intertropical Convergence Zone (ITCZ), which impacts precipitation across the globe, including the northern region of South America and the Caribbean (Waliser & Gautier, 1993; Biasutti et al., 2003).

The patterns described above are known as climate indices since the switching between phases can determine the climate of a given region; therefore, some studies try to measure the impact associated with the phenomena described by these climate indices in order to help the weather forecast in certain locations. For example, the results of Andreoli & Kayano (2007) corroborate previous studies (Moura & Shukla, 1981; Hastenrath & Greischer, 1993; Nobre & Shukla, 1996; Hastenrath, 2002) where the SAT conditions are more significant for the precipitation in Northeast Brazil (NE) than the actual dipole between NAT and SAT. These authors also report that ENSO positive (negative) phase is associated with a decrease (increase) of precipitation in the NE.

In Southern Brazil (S), Grimm et al. (2000) observed that the strongest precipitation signal is given by ENSO positive phase, with a negative trend in the year preceding the event, and positive precipitation anomalies mainly during the spring in the year of the event, attributed to circulation anomalies. Reboita et al. (2009) found that during SAM negative phase, frontogenesis and positive precipitation anomalies increase on the Southeast coast of South America while the opposite was verified for the positive phase.

Andreoli & Kayano (2005) analyzed how PDO affected rainfall in South America and reported S positive and NE negative anomalies during PDO positive phase, which would be associated with a cyclonic center on the east and NE Brazil and anticyclonic center in southeastern South America.

Giannini et al. (2004) observed signal overlap between ENSO and the Tropical Atlantic, most often during negative ENSO. Changes in the Tropical Atlantic SST force the ITCZ position in this basin, so such changes modify both sea precipitation and the annual precipitation cycle in NE (Biasutti et al., 2003).

This study aims to estimate the correlations between climate indices and precipitation in NE and S Brazil given that climate indices are important tools for assessing the effects of teleconnections on rainfall in these regions. The used indices are described in the Material and Methods section.

MATERIAL AND METHODS

The climate indices were calculated using the monthly average values of pressure and temperature at average sea level and meridional wind obtained from the NCEP (National Centers for Environmental Prediction)/NCAR (National Center for Atmospheric Research). Data spatial resolution is $2.5° \times 2.5°$, ranging

from 01/1948 to 12/2008 (Kalnay et al., 1996). Precipitation values were obtained from the GPCP (Global Precipitation Climatology Project) whose monthly averages combine satellite and station data from the period between 01/1979 and 12/2008, also with spatial resolution of 2.5° × 2.5° (Adler et al., 2003). Data can be found on the website http://www.esrl.noaa.gov/psd/. All indices were calculated, except for the PDO since the existing series extension is higher.

Calculation of the indices

El Niño-South Oscillation (ENSO)

The ENSO index is the ratio between the atmospheric component given by Southern Oscillation Index (SOI), which is the pressure difference between Tahiti and Darwin, Australia (Trenberth, 1976), and the oceanic component given by the SST anomaly in the equatorial Pacific Ocean, in Niño 3.4 area. According to Trenberth (1997), this region is located at 120°W and 170°W longitudes and the 5°S and 5°N latitudes.

In this study, SOI values were given by:

$$IOS = \frac{ST - SD}{MSD} \tag{1}$$

where

$$ST = \frac{SLMP_{Tahiti} - Mean_{Tahiti}}{\sigma_{Tahiti}} \tag{2}$$

$$SD = \frac{SLPMP_{Darwin} - Mean_{Darwin}}{\sigma_{Darwin}} \tag{3}$$

whereas $SLMP_{Tahiti}$ and $SLMP_{Darwin}$ are sea level pressure values, $Mean_{Tahiti}$ and $Mean_{Darwin}$ are the means of the studied period (1948-2008) and, σ_{Tahiti} and σ_{Darwin} are the standard deviation for Tahiti and Darwin, respectively. For the NINO3.4 index, the SST anomalies were calculated for the same area. These anomalies were obtained by removing the mean of the studied period (from 01/1948 to 12/2008) from each monthly value.

A warm ENSO is defined when the equatorial Pacific ocean SST is anomalously high and SOI is negative, that is, average sea level pressure is lower in Tahiti than in Darwin; on the contrary, a cold ENSO event corresponds to negative SST and positive SOI anomalies – SLMP in Darwin is lower than in Tahiti.

Pacific Decadal Oscillation (PDO)

PDO (Mantua et al., 1997) is defined by the SST variation in the Pacific Ocean, along with the pressure oscillation of the Aleutian Low in the North Pacific. The values given by Mantua et al. (1997) are found on the website http://jisao.washington.edu/pdo/PDO.latest. The standardized index provided by Mantua et al. (1997) is derived from analysis of the main components of SST anomalies in the North Pacific Ocean, within the range 20°N latitude to the pole. The data available is from 1900 to 2011.

Southern Annular Mode (SAM)

SAM is characterized by alternating pressure anomaly signs of the sea level in Antarctica, in the 40-50°S latitude range (Hall & Visbeck, 2002). This study followed the methodology proposed by Gong & Wang (1999):

$$SAM = P^*_{40°S} - P^*_{60°S} \tag{4}$$

where $P^*_{40°S}$ and $P^*_{60°S}$ are pressure anomalies at sea level zonally normalized for each month in the respective latitudes. The anomalies were calculated for the period of available data (1948 to 2008).

North Atlantic Oscillation (NAO)

The NAO index is defined as the pressure difference at sea level normalized by the standard deviation between the stations in Lisbon, Portugal and Stykkisholmur, Iceland, during the boreal winter (from December to March), according to Hurrell et al. (2003). The values used in this study derived from equations similar to those used to calculate SOI (Eqs. 1, 2 and 3), where NAO is given by the pressure difference between Lisbon and Stykkisholmur in this order.

Intertropical Convergence Zone (ITCZ)

The low levels of tradewinds convergence, which in equatorial latitudes results on low pressure region associated with high cloudiness, convection and precipitation, define the ITCZ (Waliser & Gautier, 1993). For simplicity, in this study the index was defined as the southern latitudes where the wind was nil, at 30°W longitude, that is, in the northeast and southeast convergence region (Servain et al., 1998, 1999). Since the exact latitude where meridional wind is zero could not be determined because only grid point data are available, the latitude with the lowest wind, that is, where it changes signal (the point closest to zero) was used. After that, the latitudes were normalized.

Atlantic Dipole Index (ADI)

The estimate of ADI given by the difference between NAT and SAT SST was calculated according to the methodology proposed by the Ocean Observation Panel for Climate (OOPC – http://ioc-goos-oopc.org/state_of_the_ocean/sur/atl/).

The monthly anomaly of SST in relation to the average of the studied period (1948-2008) was calculated for the areas between the coordinates 20°W and 40°W longitude, and 5°N and 20°N latitude; as well as between 15°W and 5°E longitude, and 5°S and 5°N latitude, for NAT and SAT, respectively.

Correlation calculations

The NE area is located within the coordinates 3°S and 16°S, and 37°W and 47°W, and S area within the coordinates 23°S and 32°S, and 48°W and 56°W. Average temporal rainfall was calculated for these areas (NE and S) from which average values and respective anomalies were determined, resulting in an average temporal precipitation anomaly for each region. Subsequently, the correlations between temporal climate indices and precipitation anomalies in the NE and S regions, without offset, were calculated. In order to check the decadal variability signal, the correlations were filtered using 120-month window moving average.

Statistical significance test used is described by Bussab & Morettin (1987) and its sequence is given below:

A. Hypothesis: the null hypothesis (H_0) considers $\rho = 0$ while the alternate hypothesis (H_1), which needs to be proven, corresponds to $\rho \neq 0$, where ρ is the population correlation coefficient.

B. Calculation of t: where r is the calculated correlation coefficient and n, sample number:

$$t = r\sqrt{\frac{n-2}{1-r^2}} \tag{5}$$

C. Critical region calculation (CR) is determined to check if the t value found for the calculated r belongs to the population at $\alpha = 5\%$ significance level. From the obtained t value from Eq. (5) and the degrees of freedom ν of the set, $\nu = n - 2$, the CR value is found in tables (Wilks, 2006). To validate the test and to reject the null hypothesis $H_0, t \in CR$.

D. Confidence interval (CI) for r is given by Fisher transformation, which transforms the correlation coefficient r into random variable normally distributed, considering $\alpha = 5\%$:

$$IC(\mu_z : 90\%) = z_0 \pm 1,96\sqrt{1/n-\nu}\,,$$
$$z_0 = \frac{1}{2}\ln\frac{1+r}{1-r}\,. \tag{6}$$

From the two z_0 values, two μ_z values are obtained:

$$e^{\mu_z} = \left(\frac{1+\rho}{1-\rho}\right)^{\frac{1}{2}} \Rightarrow e^{2\mu_z} = \frac{1+\rho}{1-\rho}\,. \tag{7}$$

When applying the two μ_z values in (7), ρ_+ and ρ_- are determined such as:

$$IC(\rho : r) =]\rho_-; \rho_+[\,. \tag{8}$$

RESULTS AND DISCUSSION

Calculated indices

The Figures from 1 to 9 show the calculated indices. The black lines represent monthly indices (except for NAO, which is yearly) while the gray lines show the series filtered by 120-month window moving average (10 years).

SOI index is shown in Figure 1. The negative values correspond to the events between 1982/83 and 1997/98, and the positives to the events between 1976/77 and 1987/88. Moreover, the intensity of the events increased from the 1970's, with higher number of events with SOI $>$ |2|. The filtered series shows a trend toward negative SOI between the decades 1970 and 2000. Figure 2 shows the NINO 3.4 index calculated for the period between 1948 and 2007. A positive trend is observed throughout the studied period, with high amplitude events from the 1970's, which is also seen in the filtered series, mainly after 1972. The positive events of 1982/83 and 1997/98 with NINO 3.4 $>$ 2 can also be observed.

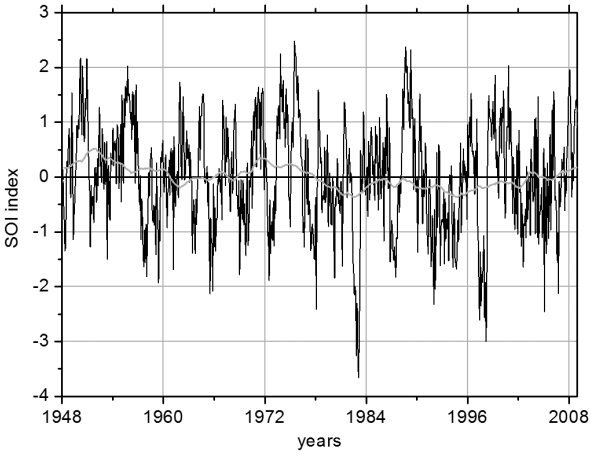

Figure 1 – Monthly SOI index (black line) and filtered values (gray line) *versus* time, in years. The filter consists of 120-month window moving average in the period from 1948 to 2008.

Figure 3 shows the PDO index from 1948 to 2008. Negative phases are seen from 1900 to 1924, from 1947 to 1976, and from 1999 on; and the positive phases from 1925 to 1946 and, from

1977 to 1998. The 1947-1976 negative phase lasted the longest. Figure 4 shows the SAM index calculated between 1948 and 2008. A negative trend is observed during the period while filtered SAM indices change from positive to negative from 1972.

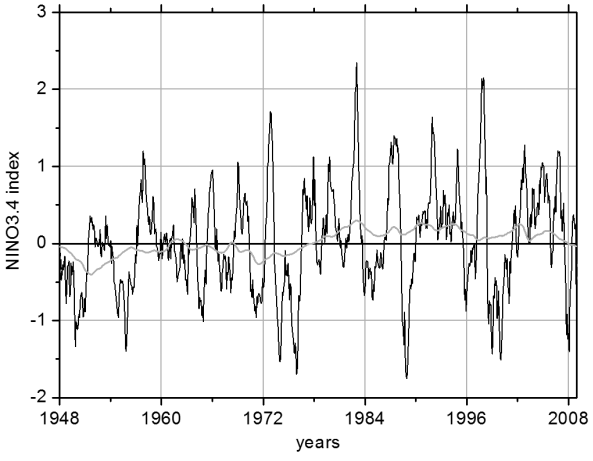

Figure 2 – Monthly NINO 3.4 index (black line) and filtered values (gray line) *versus* time, in years. The filter consists of 120-month window moving average in the period from 1948 to 2008.

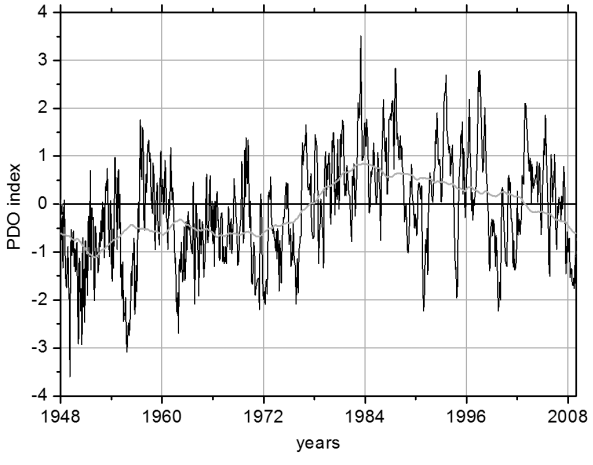

Figure 3 – Monthly PDO index (black line) and filtered values (gray line) *versus* time, in years. The filter consists of 120-month window moving average in the period from 1948 to 2008.

The NAO index characterizes an average condition during the boreal winter (December to March). Figure 5 shows the annual NAO values, from 1948 to 2007. It can be seen that the values fluctuate from one year to another while the filtered values show a low frequency oscillation characterized by a wave period of about 50 years, whose phase was inverted in the mid 70's. Figure 6 shows the ITCZ indices where it can be observed that the ITCZ yearly cycle reached up to 5°S latitude, or 2.5°N. It is noted that in most years the ITCZ reaches 1.5°N and 1°S.

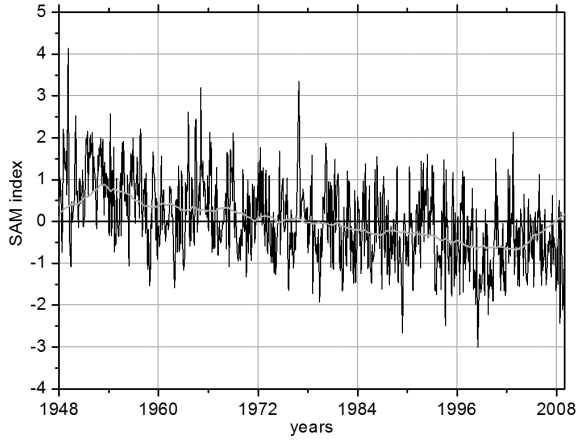

Figure 4 – Monthly SAM index (black line) and filtered values (gray line) *versus* time, in years. The filter consists of 120-month window moving average in the period from 1948 to 2008.

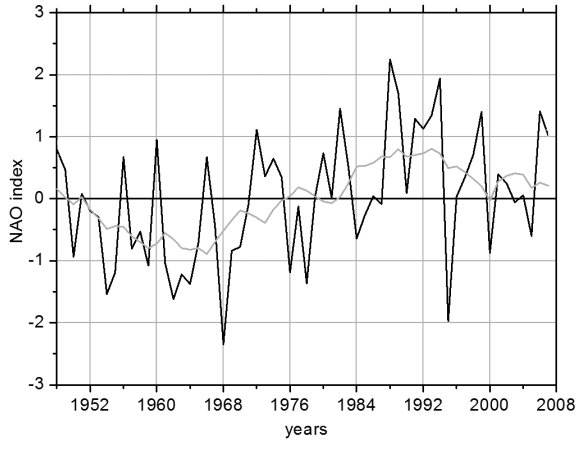

Figure 5 – Annual NAO index (black line) and filtered values (gray line) *versus* time, in years. The filter consists of 120-month window moving average in the period from 1948 to 2008.

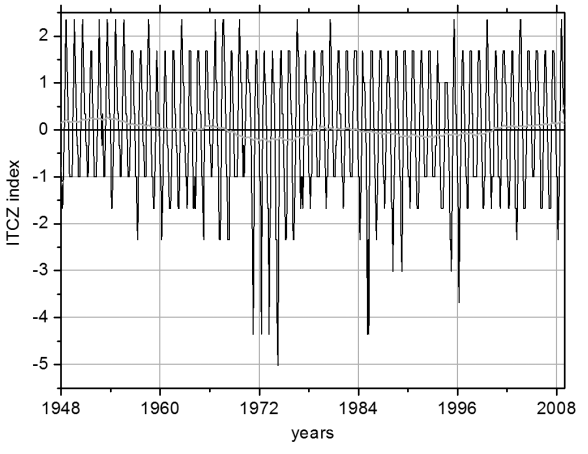

Figure 6 – ITCZ index (black line) and filtered values (gray line), in degrees (°) *versus* time, in years. The filter consists of 120-month window moving average in the period from 1948 to 2008.

The SST anomalies in the Atlantic Ocean are shown in Figures 7, 8 and 9. Both NAT (Fig. 7) and SAT (Fig. 8) data show a positive trend, which does not occur for the ADI (Fig. 9) data. An anomaly sign change is observed for both NAT and SAT in the 70 and 60's, respectively. In addition, two positive peaks are observed for the ADI data series (Fig. 9): in the late 1950's and mid 80's. The NAT data (Fig. 7) display high values in the 70's, but SAT (Fig. 8) drops about 1965.

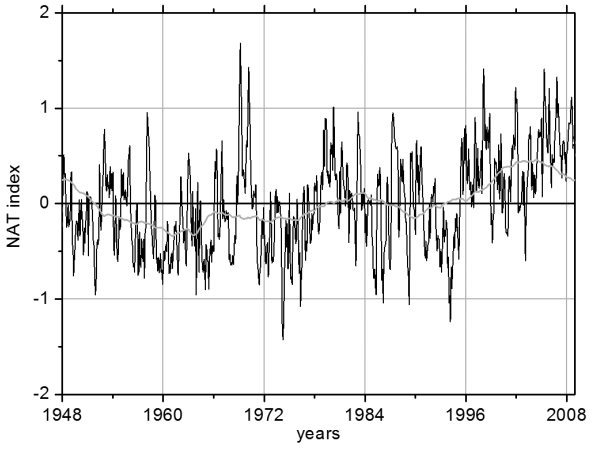

Figure 7 – NAT index (black line) and filtered values (gray line) *versus* time, in years. The filter consists of 120-month window moving average in the period from 1948 to 2008.

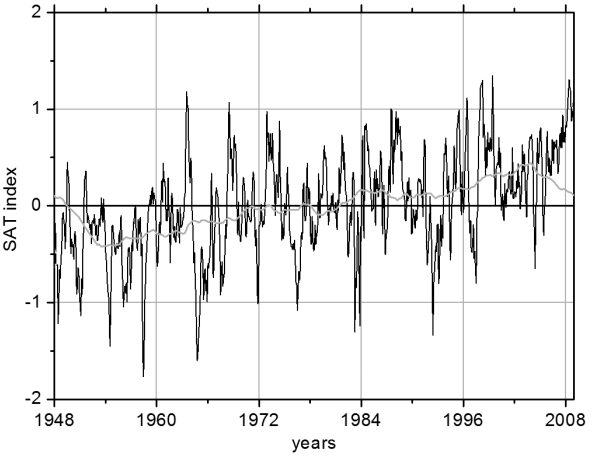

Figure 8 – SAT index (black line) and filtered values (gray line) *versus* time, in years. The filter consists of 120-month window moving average in the period from 1948 to 2008.

Temporal Precipitation Variability

ENSO is mentioned by some studies in the literature as a teleconnection phenomenon that affects the climate of NE and S Brazil (Grimm et al., 2000; Andreoli & Kayano, 2007). Thus, it is possible to compare precipitation variability between these two regions using the ENSO index. A series of cumulative monthly rainfall in the NE (Fig. 10) shows well defined annual cycle with a maximum and a minimum. Reduced precipitation can be observed in years of positive ENSO such as 1982/83 and 1997/98. During the summer months of December 1989 (negative ENSO) and January 2004 (positive ENSO) an accumulation of 370 and 388 mm, respectively, are recorded. This suggests that the ENSO index is not the only responsible for the variability of summer precipitation in the NE region.

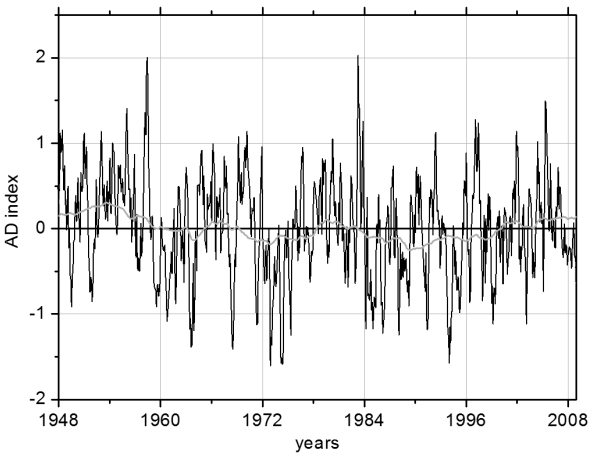

Figure 9 – AD index (black line) and filtered values (gray line) *versus* time, in years. The filter consists of 120-month window moving average in the period from 1948 to 2008.

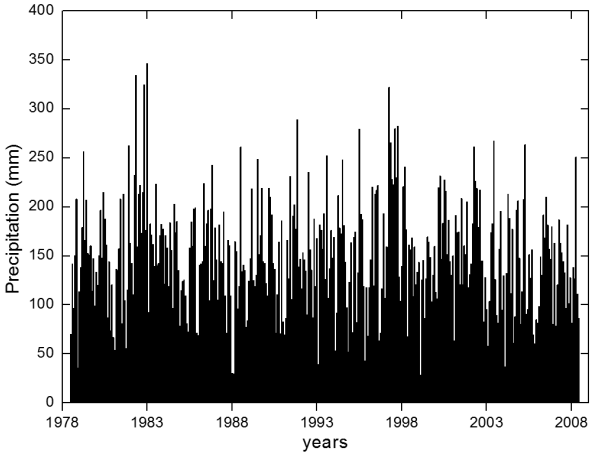

Figure 10 – Monthly rainfall (mm) for the NE region, from 1979 to 2008.

The cumulative monthly rainfall for the S region (Fig. 11) shows 346 mm in July 1983 and 322 mm in October 1997. These monthly precipitation peaks may be related to the positive ENSO events of 1982-82 and 1997-98, in addition to less pronounced annual cycle in the S region compared to the NE region.

In order to examine the low frequency variability of precipitation in the NE and S regions, both the annual cycle and trend

were removed to calculate de-seasonalized monthly anomalies. Additionally, a low-pass filter removed frequencies lower than 12 months of the resulting series. The filtered anomaly data are shown in Figures 12a (NE region) and 13a (S region). The interannual variability can be observed for both regions, with precipitation above or below the average. As an example, it is observed below average annual precipitation in the NE region and above average in the S region, during the 1982-83 period (positive ENSO). Further, the NE region displayed greater variability in the 1979-1994 period compared to 1995-2008, while in the S region the rainfall was distributed over time.

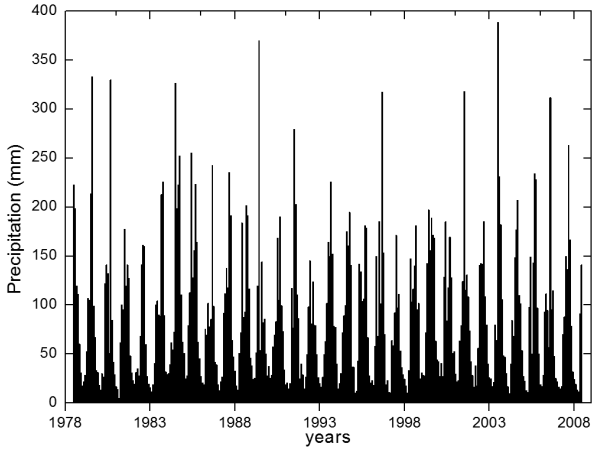

Figure 11 – Monthly accumulated rainfall (mm) for the S region, from 1979 to 2008.

Figures 12b and 13b show the wavelet spectrum applied to the filtered precipitation anomaly dataset and Figures 12c and 13c show the global wavelet spectrum, or the energy contained in each period for regions NE and S, respectively. The wavelet spectrum (Figs. 12b and 13b) indicate a possible effect of positive ENSO 1982-83 event far more important than the 1997-98 event in the NE region. On the other hand, there are energy peaks for both events in the S region. However, the 1982-83 event had a more prolonged effect than the 1997-98. The wavelet analysis corroborates the behavior of precipitation variability observed in Figures 12a and 13a, a greater amount of energy is observed in 1979-1994 period compared to 1995-2008 in the NE while in the S, the energy is distributed over time.

The energy peak in the interannual band (from 3 to 7 years, possibly connected to ENSO) was significant in the NE with 85% confidence. In the S, the interannual band was significant with 90% confidence (Fig. 13c). These results point to a significant influence of interannual variability in both regions, NE and S.

Correlation analysis

Correlation analysis between climate indices and rainfall data was performed in two steps. The first consisted of calculating the correlation coefficient between climate indices and rainfall over time in the regions NE and S, without offset and filters. The second step consisted of a similar procedure where both datasets (indices and precipitation) were filtered using the 120-month window moving average (10 years).

Correlation of non-filtered series

For the unfiltered correlation (Table 1), the highest observed value is 0.26, which corresponds to the ratio between precipitation in the S and the NINO3.4 index. The most negative correlation is between the SOI index and precipitation in the S, suggesting that ENSO is the main variability factor for the S. Generally, the correlation between all indices and precipitation in the NE and S is low with opposite sign; however, the effect of some phenomena is more significant in one region compared to the other. The phenomena AD, SAT, NINO3.4, SOI and PDO cause more impact on the S compared to NE while NAO and ITCZ impact more the NE.

The results of the correlation analysis for filtered data (Table 2) are different than the results of unfiltered data shown in Table 1. An amplified impact of weather patterns is observed on the precipitation in the NE and S regions. The most important relationship obtained is between the NE precipitation and the SOI index (0.81), which can be connected with changes in atmospheric pressure field. Rainfall in the S has a negative correlation (–0.30), suggesting an opposite relationship between SOI and precipitation in the S and NE. The NINO 3.4 index has a negative correlation with precipitation in both regions NE (–0.46) and S (–0.27); however, it is suggested that the SOI impact prevails since there are studies suggesting an inverse correlation for the ENSO impact on the N and SE (e.g. Garreaud et al., 2009). The correlation between the NE precipitation and the NAO index is also highlighted (–0.63) corroborating the study of Giannini et al. (2001), who suggests a negative correlation between NAO and precipitation in Central America and in the northern region of South America. These authors state that this correlation is indirect and occurs due to SST anomalies associated with the tropical surface winds and anomalous subsidence.

The impact of ITCZ on the NE precipitation (e.g. Biasutti et al., 2003) is confirmed by the resulting correlation (0.50), suggesting that the ITCZ presence over the NE increases rainfall. The position of ITCZ to the south of the equator from March to May defines the rainy season in northern NE as the cloud band

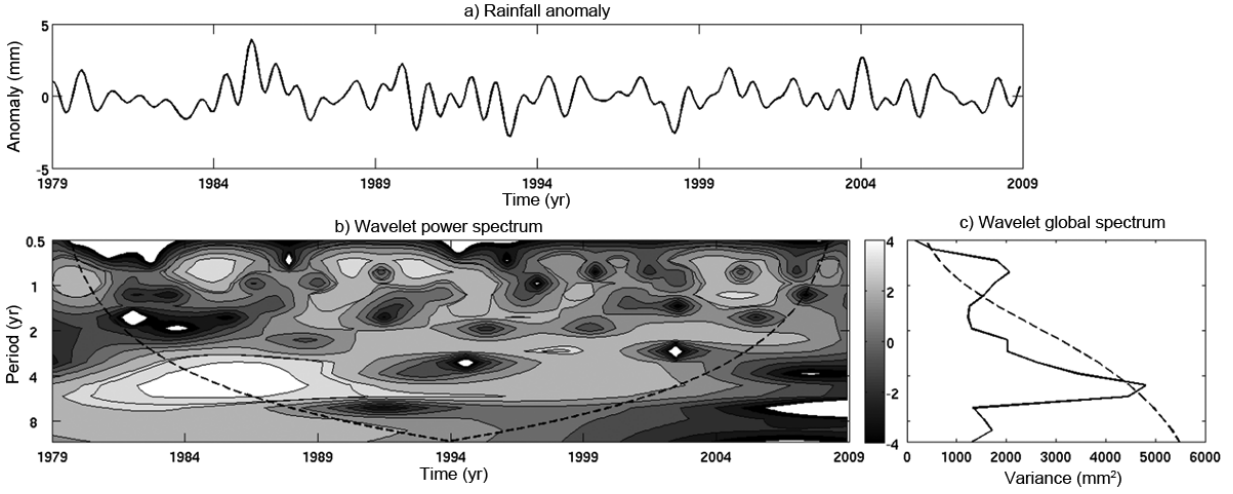

Figure 12 – a) de-seasonalized anomalies with no trends for the NE region, in mm, from which it was removed high frequency greater than or equal to 12 months by means of low-pass filter. b) wavelet power spectrum using Morlet wavelet-mother, in mm. The dashed line delimits the cone of influence (below this line, the results are not reliable because they are influenced by edge effects). c) wavelet global spectrum. The solid line represents variance, in mm^2, and the dashed line represents the theoretical spectrum with confidence of 85%.

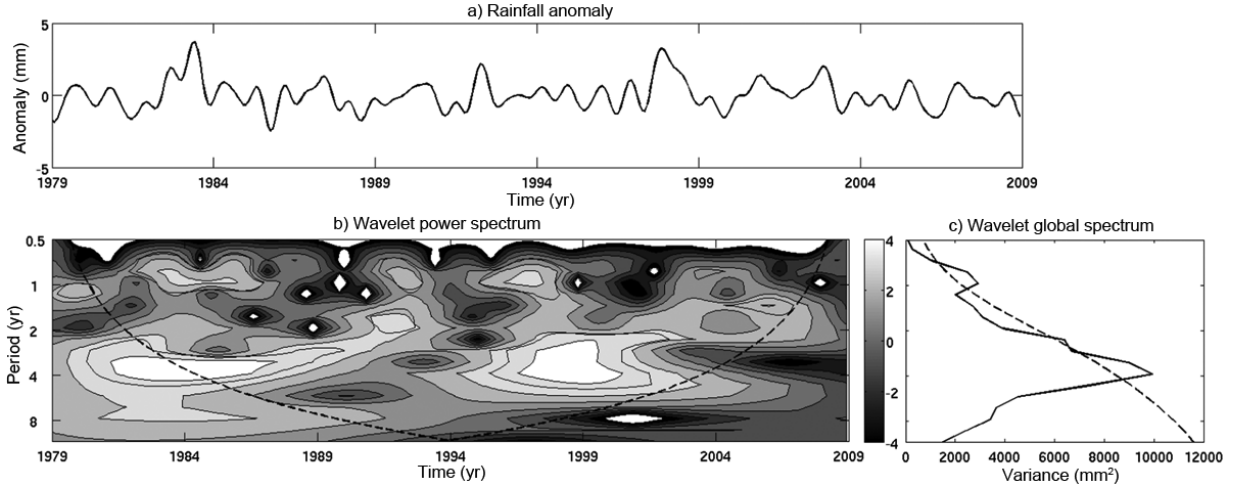

Figure 13 – a) de-seasonalized anomalies with no trends for the S region, in mm, from which it was removed high frequency greater than or equal to 12 months by means of low-pass filter. b) wavelet power spectrum using Morlet wavelet-mother, in mm. The dashed line delimits the cone of influence (below this line, the results are not reliable because they are influenced by edge effects). c) wavelet global spectrum. The solid line represents variance, in mm^2, and the dashed line represents the theoretical spectrum with confidence of 90%.

moves over the region bringing cumulative rainfall. The impact of PDO is greater on precipitation in the S (–0.20) compared to the NE (–0.04), which may be related to the extratropical nature of the PDO (Mantua et al., 1997). SAM index has a higher correlation with precipitation in the S compared to the NE, and this result reflects the importance of SAM on the formation of cyclogenetic systems, which are primarily responsible for precipitation in the S (Reboita et al., 2008). The indices NAT and SAT are positively correlated with precipitation in the NE (0.35; 0.37) and S (0.36; 0.29) and the importance of the Tropical Atlantic SST dipole, represented by the correlation with the ADI index, is more significant in the S (0.41). These figures show that higher Tropical Atlantic SST cause above average precipitation in the S. It is worth noting that these results are related to decadal frequency only, which does not exclude possible correlation among sets in other time scales.

Table 1 – Pearson correlation coefficient obtained for the NCEP data climate indices and the GPCP precipitation anomalies, for unfiltered and without offset (offset 0) series.

Area	SAM	NAT	SAT	ADI	Nino3.4	SOI	PDO	NAO	ITCZ
NE	–0.05	–0.03	0.05	–0.07	–0.14	0.08	–0.04	–0.13	–0.11
S	0.05	0.04	–0.13	0.13	0.26	–0.17	0.15	0.08	0.02

Table 2 – Pearson correlation coefficient obtained for the NCEP data climate indices and the GPCP precipitation anomalies (1979-2008), without offset (offset 0), from values filtered using 120-month window moving average.

Area	SAM	NAT	SAT	ADI	Nino3.4	SOI	PDO	NAO	ITCZ
NE	–0.05	0.35	0.37	0.29	–0.46	0.81	–0.04	–0.63	0.50
S	0.48	0.36	0.29	0.41	–0.27	–0.30	–0.20	–0.19	0.19

The analysis of the average monthly precipitation between 1911 and 1989 performed by Wainer & Soares (1997) shows significant decadal variability. These authors found that the relations between SST, precipitation in NE and the pseudo-meridional wind stress in the decadal scale are similar to the interannual and seasonal scales. In both time scales, the Tropical Atlantic SST is in phase with the meridional displacement of the Intertropical Convergence Zone and associated pseudo-meridional wind stress and out of phase with precipitation.

The lower correlation between the Tropical Atlantic and precipitation in NE compared to the correlation with the S (AD index) may be explained by the results of Wainer et al. (2008). This work shows that decadal variability of tropical Atlantic Ocean prevails only in part of the 130-year record (1880 to 1920) suggesting that decadal variability of tropical Atlantic is episodic rather than a periodic oscillation.

The correlation values between precipitation and NAO and ITCZ indices, as well as precipitation in S and the SAM index were tested using t-Student test (Bussab & Morettin, 1987) despite being less than $|0.75|$ since previous works have indicated a correlation among them (e.g. Horel et al., 1989, for the ITCZ). The test validated the correlation between NAO index and precipitation in NE, but the confidence interval computed for the correlation coefficient ($r = -0.63$) did not contain it $\left(IC(r = -0.63) =]0.75; 0.92[\right)$. It was concluded that the relationship has not been established due to the small sample size since the NAO index had annual figures for a total of only 29 years. The correlation analysis between precipitation in the NE and the ITCZ index ($r = 0.50$) was validated by the t-Student test and the correlation coefficient was within the confidence interval $\left(IC(r = 0.50) =]-0.68; 0.96[\right)$. However, the confidence interval is quite large thus decreasing its reliability. The correlation between precipitation in the S and the SAM index ($r = -0.48$) was also validated by the t-test with a quite large confidence interval $\left(IC(r = -0.48) =]-0.96; 0.70[\right)$ and questionable reliability.

CONCLUSIONS

The correlations obtained for unfiltered series were low, but revealed some significant relationships such as the impact of ENSO on the NE and S precipitation with opposite sign.

The decadal analysis of the correlation of data filtered using a 120-month window moving average was more indicative of the effects of some indices on the rainfall in the NE and S regions. In the NE region, the most significant correlation was obtained for NINO 3.4 and SOI (ENSO) indices, which represent the ENSO phenomena and correspond to 21% and 65% of variance, respectively. The highest correlation of the SOI index suggests greater engagement of the pressure field, which causes changes in the equatorial circulation during ENSO episodes.

The precipitation in the NE was also dependent on the NAO and ITCZ with variance explained by the corresponding indices of 40% and 25%. The NAO result is not considered significant because it was not validated by the t-test probably due to insufficient data for the correlation to be reliable.

The SAM and ADI indices were the best correlated with the filtered precipitation dataset in decadal scale, thus explaining 23% and 17% of precipitation variability, respectively, in the S region. Thus, the positive SAM index characterizes higher surface pressures in the 40°S latitude, which is not favorable for the cyclogenesis in the S and, therefore, decreases precipitation since the correlation between SAM and precipitation is negative in the S. The positive correlation for the ADI index indicates that TNA SST (Tropical North Atlantic Sea Surface Temperature)

higher than TSA SST (Tropical South Atlantic Sea Surface Temperature) favors precipitation in the S region. In general, above average SST across the Tropical Atlantic favors precipitation in the S by increasing moisture from the ocean to the continent, which is transported to the S by low level jet.

Although it accounts for only 4% of rainfall variability, the PDO index was more significant for the precipitation in the S compared to the NE region. The negative correlation indicates above average rainfall in the periods of negative PDO index. Andreoli & Kayano (2005) assigned positive precipitation anomalies in the S during PDO positive phases to the strengthened subtropical jet associated with a cyclonic system at surface.

Spectral analysis of the data filtered for low frequencies showed that interannual variability corresponds to the primary frequency in the global spectrum of precipitation wavelets of the NE and S regions, with 85% and 90% significance, when removed the annual cycle. Moreover, several behavior patterns of more intense positive ENSO events were observed in the studied period (1982-83 and 1997-98) in the NE region, while in the S both events caused above average rainfall.

Overall the results suggest that the teleconnection patterns influence precipitation in the NE and S regions, at decadal time scale. However, the length of the precipitation series used (30 years) may not be sufficient to show the decadal variability of the studied parameters. In this regard, further research is suggested using a longer precipitation series with higher resolution (e.g. CPC, Chen et al., 2002). Nevertheless, considering the consistency with previous results, the correlations show strong indications of the possible impact of some of the phenomena represented by the climate indices. In addition, it is necessary to extend the investigation of physical mechanisms that operate in these interactions in order to contribute to climate forecast in these regions, in decadal time scale.

ACKNOWLEDGMENTS

The software used to calculate the wavelets was provided by C. Torrence and G. Compo, and is available on the website http://atoc.colorado.edu/research/wavelets/.

REFERENCES

ADLER RF, HUFFMAN GJ, CHANG A, FERRARO R, XIE P, JANOWIAK J, RUDOLF B, SCHNEIDER U, CURTIS S, BOLVIN D, GRUBER A, SUSSKIND J & ARKIN P. 2003. The Version 2 Global Precipitation Climatology Project (GPCP) Monthly Precipitation Analysis (1979-Present). J. Hydrometeorol., 4: 1147–1167.

ANDREOLI RV & KAYANO MT. 2005. ENSO-related rainfall anomalies in South America and associated circulation features during warm and cold Pacific Decadal Oscillation regimes. Int. J. Climatol., 25: 2017–2030.

ANDREOLI RV & KAYANO MT. 2007. A importância relativa do Atlântico tropical sul e Pacífico leste na variabilidade de precipitação do Nordeste do Brasil. Rev. Bras. Meteorol., 22(1), doi: 10.1590/S0102-77862007000100007.

BIASUTTI M, BATTISTI DS & SARACHIK ES. 2003. The annual cycle over the Tropical Atlantic, South America, and Africa. J. Climate, 16: 2491–2508.

BJERKNES J. 1966. A possible response of the atmospheric Hadley circulation to equatorial anomalies of ocean temperature. Tellus, 18: 820–829.

BUSSAB WO & MORETTIN PA. 1987. Métodos quantitativos – Estatística básica. 4th ed., Atual Editora, São Paulo, 321 pp.

CHEN M, XIE P, JANOWIAK JE & ARKIN PA. 2002. Global Land Precipitation: A 50-yr monthly analysis based on gauge observations. J. Hydrometeorol., 3: 249–266.

GARREAUD RD, VUILLE M, COMPAGNUCCI R & MARENGO J. 2009. Present-day South American climate. Palaeogeogr. Palaeocl., 281: 180–195.

GIANNINI A, CANE MA & KUSHNIR Y. 2001. Interdecadal changes in the ENSO teleconnection to the Caribbean region and the North Atlantic Oscillation. J. Climate, 14: 2867–2879.

GIANNINI A, SARAVANAN R & CHANG P. 2004. The preconditioning role of Tropical Atlantic Variability in the development of the ENSO teleconnection: implications for the prediction of Nordeste rainfall. Clim. Dynam., 22(8): 839–855.

GONG D & WANG S. 1999. Definition of the Antarctic oscillation index. Geophys. Res. Lett., 26: 459–462.

GRIMM AM. 2003. The El Niño impact on the summer monsoon in Brazil: regional processes *versus* remote influences. J. Climate, 16: 263–280.

GRIMM AM, BARROS VR & DOYLE ME. 2000. Climate variability in southern South America associated with El Niño and La Niña events. J. Climate, 13: 35–58.

HALL A & VISBECK M. 2002. Synchronous variability in the Southern Hemisphere atmosphere, sea ice, and ocean resulting from the annular mode. J. Climate, 15: 3043–3057.

HASTENRATH S. 2002. Dipoles, temperature gradients, and tropical climate anomalies. B. Am. Meteorol. Soc., 83: 735–738.

HASTENRATH S & GREISCHER L. 1993. Further work on the prediction of Northeast Brazil rainfall anomalies. J. Climate, 6: 743–758.

HASTENRATH S & HELLER L. 1977. Dynamics of climatic hazards in northeast Brazil. Q. J. Roy. Meteor. Soc., 103(435): 77–92.

HOREL JD, HAHMANN AN & GEISLER JE. 1989. An investigation of the annual cycle of convective activity over the tropical Americas. J. Climate, 2: 1388–1403.

HURRELL JW, KUSHNIR Y, OTTERSEN G & VISBECK M. 2003. The North Atlantic Oscillation: climatic significance and environmental impact. Geophysical Monograph Series, Washington, DC: American Geophysical Union. v. 134, 279 pp.

KALNAY E, KANAMITSU M, KISTLER R, COLLINS W, DEAVEN D, GANDIN L, IREDELL M, SAHA S, WHITE G, WOOLEN J, ZHU Y, LEETMAA A, REYNOLDS R, CHELLIAH M, EBISUZAKI W, HIGGINS W, JANOWIAK J, MO KC, ROPELEWSKI C, WANG J, JENNE R & JOSEPH D. 1996. The NCEP/NCAR 40-year reanalysis project. B. Am. Meteorol. Soc., 77: 437–470.

MANTUA NJ, HARE SR, ZHANG Y, WALLACE JM & FRANCIS RC. 1997. A pacific interdecadal climate oscillation with impacts on salmon production. B. Am. Meteorol. Soc., 78(6): 1069–1079.

MOURA AD & SHUKLA J. 1981. On the dynamics of droughts in Northeast Brazil: observations, theory and numerical experiments with a general circulation model. J. Atmos. Sci., 38: 2653–2675.

NOBRE P & SHUKLA J. 1996. Variations of sea surface temperature, wind stress and rainfall over the Tropical Atlantic and South America. J. Climate, 10(4): 2464–2479.

REBOITA MS, AMBRIZZI T & ROCHA RP. 2009. Relationship between the Southern Annular Mode and Southern Hemisphere atmospheric systems. Rev. Bras. Meteorol., 24(1): 48–55.

SERVAIN J, WAINER I, DESSIER A & McCREARY JP. 1998. Modes of climatic variability in the tropical Atlantic. In: SERVAT E, HUGHES D, FRITSCH J-M & HULME M (Eds.). Water Resources Variability in Africa in the 20th Century (Proc. Conf. IAHS), 45–55.

SERVAIN J, WAINER I, McCREARY Jr JP & DESSIER A. 1999. Relationship between the equatorial and meridional modes of climatic variability in the tropical Atlantic. Geophysical Research Letters, 26: 485–488.

SERVAIN J, CLAUZET G & WAINER I. 2003. Modes of Tropical Atlantic variability observed by PIRATA. Geophys. Res. Lett., 30(5), 8003, doi: 10.1029/2002GL015124.

TRENBERTH KE. 1976. Spatial and temporal variations of the Southern Oscillation. Q. J. Roy. Meteor. Soc., 102: 639–653.

TRENBERTH KE. 1997. The definition of El Niño. B. Am. Meteorol. Soc., 78(12): 2771–2777.

VAN LOON H & ROGERS JC. 1978. The seesaw in winter temperatures between Greenland and Northern Europe. Part I: General description. Mon. Wea. Rev., 106: 296–310.

WAINER I, CLAUZET G & SERVAIN J. 2003. Time scales of upper ocean temperature variability inferred from the PIRATA data (1997-2000). Geophys. Res. Lett., 29, doi: 10.1029/2002GL015147.

WAINER I, SERVAIN J & CLAUZET G. 2008. Is the decadal variability in the tropical Atlantic a precursor to the NAO? Ann. Geophys., 26(12): 4075–4080.

WAINER I & SOARES J. 1997. North-northeast Brazil rainfall and its decadal scale relationship to wind stress and sea surface temperature. Geophys. Res. Lett., 24: 277–280.

WALISER D & GAUTIER C. 1993. A Satellite-derived climatology of the ZCIT. J. Climate, 6: 2162–2174.

WALKER GT. 1928. Ceará (Brazil) Famines and the general circulation movements. Beitr. Phys. Atmos., 14: 88–93.

WALLACE JM & GUTZLER DS. 1981. Teleconnections in the geopotential height field during the Northern Hemisphere winter. Mon. Wea. Rev., 109: 784–812.

WILKS DS. 2006. Statistical methods in the atmospheric sciences. International Geophysics Series, 2nd ed., 627 pp.

Recebido em 24 junho, 2011 / Aceito em 30 janeiro, 2012
Received on June 24, 2011 / Accepted on January 30, 2012

NOTES ABOUT THE AUTHORS

Luciana Figueiredo Prado is a PhD student of Physical Oceanography at the Oceanographic Institute of the Universidade de São Paulo (USP-IO). BS and Master of Science in Meteorology from the Institute of Astronomy, Geophysics and Atmospheric Sciences, Universidade de São Paulo (IAG-USP). The area of interest is Climatology and Ocean-Atmosphere Interaction. The doctoral research project aims to investigate the ocean-atmosphere interaction in the South Atlantic Ocean and hydrological paleocycle in eastern subtropical South America during the Holocene.

Ilana Wainer is a tenured professor in the Department of Physical Oceanography at the Oceanographic Institute of the Universidade de São Paulo. Specialist in ocean-atmosphere interaction and climate using coupled models of high complexity. Participates in the INCT-Cryosphere committee, researches climate modeling to understand the role of sea ice and ice shelves in the Antarctic Ocean circulation and climate impact. In addition to extensive teaching and research activity, participates in international program committees such as the World Climate Research Program (WCRP), and as a physical oceanography specialist in the SCAR (Scientific Committee for Antarctic Research) workgroup. Currently is vice chairman of the executive committee of the Scientific Committee for Ocean Research (SCOR).